Single-mode dynamics of convective instabilities in a horizontal liquid layer

Vittorio Degiorgio*
Centro Informazioni Studi Esperienze, Via Reggio Emilia Segrate, 20090 Milano, Italy
(Received 26 March 1979)

A theoretical description of the single-mode dynamics of both the Rayleigh-Bénard instability (RBI) and the Soret-driven instability (SDI) is provided, starting from the general conservation equations and exploiting a technique similar to that used for the laser instability. A system of nonlinear dynamic equations is found to describe self-consistently both the RBI and the SDI. The single-mode steady-state solutions are derived without making use of perturbation expansions. A quantitative theoretical explanation is found to account for such recent experimental results as the saturation of the horizontally averaged concentration gradient at midheight in the SDI, the appearance of relaxation oscillations in RBI and SDI transients, and the dependence of the oscillation period on the temperature difference between the plates. The analogy with the laser suggests the possibility of observing giant pulses in the transient well above threshold, and of measuring pretransitional fluctuations of the mode which goes unstable. Connections with the Lorenz model are also discussed.

I. INTRODUCTION

Convective phenomena have been actively studied for a long time because of their importance in many branches of applied research. The consideration that the convective instability may be viewed, near its threshold, as an example from the large class of instabilities in open systems showing a close analogy to phase transitions in thermodynamic systems, has stimulated in the last few years a considerable amount of experimental and theoretical work. Many results have been obtained concerning the steady state, less is known however about the transient behavior of convective instabilities. The aim of this paper is to provide a theoretical description of the single-mode dynamics of both the Rayleigh–Bénard instability (RBI) and the Soret-driven instability (SDI), starting from the general conservation equations and exploiting a technique similar to that used for the laser instability.[1]

The RBI arises in thin horizontal liquid layers heated from below when the temperature difference ΔT across the layer exceeds a critical value ΔT_c.[2-5] The less well-known SDI may occur in two-component fluid layers, above a critical temperature difference, when the direction of the heat flux in the layer and the sign of the thermal diffusion ratio k_T are such that the molecules of the heavier component migrate upwards.[6-8] The thermal diffusion ratio is defined through the relation[9]

$$\text{grad}\, c = -(k_T/T)\text{grad}\, T\ ,$$

where c is the mass fraction of the heavier component and T is the absolute temperature. More commonly the heavier component migrates toward the colder plate of the Soret cell, that is $k_T > 0$.

Whereas the driving force of the RBI is due to the density gradient created by the applied temperature gradient, the driving force of the SDI comes from that part only of the density gradient which is due to the concentration gradient originated by thermal diffusion. As discussed in Ref. 7 this phenomenon arises because the relaxation time for heat is much smaller than the corresponding time for mass, in liquid mixtures. Only recently experimental evidence of the SDI has been presented.[10-12]

The treatment presented here is limited to the region not too far above threshold where a single-mode convection pattern sets in. The single-mode treatment has the virtue of splitting the complicated space-time-dependent problem into two separate problems. The spatial structure is specified by solving in the space domain a system of two linear time-independent equations with boundary conditions dictated by the geometry of the cell and by the external constraints. The time evolution of the single-mode amplitudes is given by a set of space-independent equations. This approach, successfully applied in the laser theory,[13] is of quite general validity for the threshold region of instabilities in open systems.[14] It should be noted that the assumption of fixed spatial structure of the convection pattern was first made in hydrodynamics by Stuart,[15] and it is known indeed as the "Stuart shape assumption." However, this assumption has never been exploited with the aim to derive a self-consistent set of dynamic equations, as is done in this work.

The organization of the paper is as follows. Considering first the RBI case, I derive in Sec. II the nonlinear dynamic equations for the single-mode amplitudes of the velocity and temperature mode and for the horizontally averaged temperature gradient. The same set of equations is shown

successively to apply also to the SDI variables which are the single-mode amplitudes of the velocity and concentration mode and the horizontally averaged concentration gradient.

The steady-state solutions are derived in Sec. III from the self-consistent equations without making use of perturbation expansions. Besides other results, it is found that the temperature gradient (concentration gradient for the SDI) at the midplane of the cell takes, above threshold, a value independent of ΔT and coincident with the critical temperature (concentration) gradient. This saturation effect is a new theoretical result, and it has indeed been observed in the SDI experiment of Ref. 11.

The transient evolution of the instability toward the steady state starting from an arbitrary initial condition at $t=0$ is discussed in Sec. IV. The system of three equations derived in Sec. II is simplified by an adiabatic elimination of the velocity which is taken to be the variable evolving on the fastest time scale. This approximation is valid for the RBI in large-Prandtl-number fluids and is generally valid for the SDI in liquid mixtures. The obtained couple of "rate equations" is solved numerically, and the solutions are compared with the results of recent experiments on the dynamics of the RBI[16-19] and of the SDI.[12]

Finally, Sec. V considers the connections with the Lorenz model[20] and describes the analogy with the laser. *A posteriori*, the analogy is not all surprising if one takes into account that the model presented in this paper can be viewed upon as a generalization of the Lorenz model to a nonsinusoidal vertical dependence of the mode amplitudes, and one further recalls the analogy between the Lorenz model and the laser suggested in Ref. 21. Since the velocity is the variable analogous to the electric field in the laser model, the adiabatic elimination which produces the instability rate equations is analogous to the approximation introduced by Bonifacio and Schwendimann[22] to describe superradiant pulses. The possibility of observing in convective-instability experiments superradiant pulsing phenomena will be discussed shortly. The analogy with the laser suggests also that a measurement of the statistical properties[23] of convective instability transient could give information on fluctuations near the instability threshold.

II. SINGLE-MODE DYNAMIC EQUATIONS

The well-known conservation equations for a two-component liquid mixture are[7]

$$\frac{\partial c}{\partial t}+\sum_{j=1}^{3} v_j \frac{\partial c}{\partial x_j}=D\nabla^2 c+\frac{Dk_T}{\overline{T}}\nabla^2 T\,, \tag{1}$$

$$\frac{\partial v_i}{\partial t}+\sum_{j=1}^{3} v_j \frac{\partial v_i}{\partial x_j}=g[1-\alpha(T-\overline{T})+\gamma(c-\overline{c})]\lambda_i - \frac{1}{\overline{\rho}}\frac{\partial p}{\partial x_i}+\nu\nabla^2 v_i\,, \tag{2}$$

$$\frac{\partial T}{\partial t}+\sum_{j=1}^{3} v_j \frac{\partial T}{\partial x_j}=\chi\nabla^2 T\,, \tag{3}$$

$$\sum_{j=1}^{3}\frac{\partial v_j}{\partial x_j}=0\,, \tag{4}$$

where c is the mass fraction of the heavier component, v_i is the ith component of the velocity, T the temperature, and p the pressure. The constant D represents the isothermal diffusion coefficient, ν the kinematic viscosity, χ the thermal diffusivity, g the gravity acceleration, $\alpha=-(1/\rho)(\partial\rho/\partial T)$, and $\gamma=(1/\rho)(\partial\rho/\partial c)$, where ρ is the density. The symbols $\overline{T},\overline{c},\overline{\rho}$ represent average quantities over the layer. Taking the z axis ($i=3$) coincident with the vertical axis, $\lambda_i=0$ for $i=1,2$, and $\lambda_3=1$. A discussion of the assumptions involved in the derivation of Eqs. (1)–(4) can be found, for instance, in Ref. 7. The equations for a single-component system are immediately obtained from Eqs. (1)–(4) by putting $c=\overline{c}=0$.

A. Rayleigh-Bénard instability

The treatment is limited to the region not too far above threshold where a single-mode convection pattern sets in. Following the single-mode assumption, the vertical component of the velocity v_z and the temperature T are expressed as

$$v_z=B(t)v(z)\cos(\vec{k}\cdot\vec{r})\,, \tag{5}$$

$$T=\overline{T}+A(z,t)+T(t)\theta(z)\cos(\vec{k}\cdot\vec{r})\,, \tag{6}$$

where the origin of the coordinates system is put in the center of the cell, $\vec{r}$ designates an horizontal vector in the configuration space, and $\vec{k}$ is the corresponding wave number. Equations (5) and (6) differ from the positions made in classical linear-mode analysis because the time dependence of velocity and temperature is not exponential, and $A(z,t)$ which represents the average over the horizontal plane of the reduced temperature $T-\overline{T}$ is not assumed *a priori* to be a linear function of z. In fact, when ΔT exceeds the critical value ΔT_c, a z-dependent convective heat flux is generated in the liquid layer. Consequently, the temperature gradient cannot stay constant over the cell height.

The dimensionless functions $v(z)$ and $\theta(z)$ are taken here as known functions. They are indeed the solutions of the eigenvalue problem which defines the neutral stability curve. To be precise, $v(z)$ satisfies the linear equation[2]

$$k^4a^4\left(\frac{1}{k^2}\frac{d^2}{dz^2}-1\right)^3 v(z)=-Rv(z)\,, \tag{7}$$

where a is the gap between the horizontal plates confining the fluid layer, and $R = g\alpha\Delta T a^3/\nu\chi$ is the Rayleigh number. An identical equation governs $\theta(z)$. If both bounding surfaces are rigid (this is the only case considered in the present paper), the appropriate boundary conditions are

$$\frac{dv}{dz} = v(z) = 0 \quad \text{for } z = \pm\tfrac{1}{2}a . \tag{8}$$

Furthermore, if the two surfaces are maintained at fixed temperatures,

$$\theta(z) = 0 \quad \text{for } z = \pm\tfrac{1}{2}a . \tag{9}$$

Another possible situation is that of fixed heat flux through the layer. In this latter case, instead of Eq. (9) the appropriate boundary condition is

$$\frac{d\theta}{dz} = 0 \quad \text{for } z = \pm\tfrac{1}{2}a . \tag{10}$$

The two functions $v(z)$ and $\theta(z)$ take their maximum value at the midplane $z = 0$. I assume that $v(0) = \theta(0) = 1$, without loss of generality since the dependence on the temperature difference ΔT can be included into the time-dependent amplitudes $B(t)$ and $T(t)$.

By applying conditions (8) and (9), the minimum of the marginal stability curve is attained at $k_c = 3.117/a$, where $R_c = 1708$. The corresponding solutions $v(z)$ and $\theta(z)$ can be found, for instance, on p. 39 of Ref. 2.

Consistently with the single-mode approach, $A(z,t)$ can be written

$$A(z,t) = -(\Delta T/a)z + A(t)f(z) , \tag{11}$$

where the dimensionless function $f(z)$ is determined by considering that, at steady state,

$$\frac{1}{a}\frac{d(v\theta)}{dz} = \frac{d^2 f}{dz^2} , \tag{12}$$

and that $f(z) = 0$ for $z = 0, \pm\frac{1}{2}a$. The integration of Eq. (12) yields

$$f(z) = -\left(\frac{2z}{a} + 1\right)\int_{-a/2}^{0} \frac{v\theta}{a}dz + \int_{-a/2}^{z} \frac{v\theta}{a}dz . \tag{13}$$

I assume now that $\vec{k}$ is parallel to the x axis. Clearly all variables become independent of y. The horizontal velocity component v_x, as derived from Eqs. (5) and (6), reads

$$v_x = -\frac{B(t)}{k}\frac{dv}{dz}\sin kx . \tag{14}$$

By substituting Eqs. (5),(6),(11), and (14) into Eq. (3) and averaging over the horizontal plane, the following two equations are obtained:

$$\frac{dA}{dt}f + \frac{BT}{2}\left(\frac{dv}{dz}\theta + v\frac{d\theta}{dz}\right) = \chi A\frac{d^2 f}{dz^2} , \tag{15}$$

$$\frac{dT}{dt}\theta = \left(\frac{\Delta T}{a} - A\frac{df}{dz}\right)Bv + \chi T\left(\frac{d^2\theta}{dz^2} - k^2\theta\right) . \tag{16}$$

By integrating both sides of Eq. (15) from $z = -\frac{1}{2}a$ to $z = 0$, by putting $z = 0$ in Eq. (16) and by introducing the new variable

$$\Delta(t) = \frac{\Delta T}{a} - A(t)\left(\frac{df}{dz}\right)_{z=0} ,$$

Eqs. (15) and (16) become

$$\dot{\Delta} = -[h_1/(2a^2)]BT - (h_2\chi/a^2)(\Delta - \Delta_0) , \tag{17}$$

$$\dot{T} = \Delta B - h_3\chi k^2 T , \tag{18}$$

where $\Delta_0 = \Delta T/a$, and the dimensionless positive constants h_1, h_2, h_3 depend only on $v(z)$, $\theta(z)$, and on the product ka, and are expressed as

$$h_1 = -a^2\frac{(df/dz)_{z=0}}{\int_{-a/2}^{0} f\,dz} , \tag{19}$$

$$h_2 = -a^2\frac{\int_{-a/2}^{0}(d^2 f/dz^2)dz}{\int_{-a/2}^{0} f\,dz} , \tag{20}$$

$$h_3 = 1 - \frac{1}{k^2}\left(\frac{d^2\theta}{dz^2}\right)_{z=0} . \tag{21}$$

It should be pointed out that the elimination of the spatial dependence from the dynamic equations presents some degree of arbitrariness. I have chosen a local evaluation of Eq. (16) instead of an average over the interval $(-\frac{1}{2}a, 0)$ only because it is the most direct way to introduce the variable $\Delta(t)$ which represents the temperature gradient, averaged over the horizontal plane, at $z = 0$.

The system of Eqs. (17) and (18) is completed by a third equation which is derived from Eq. (2) with $c = \bar{c} = 0$, by eliminating the pressure p as follows:

$$\begin{aligned}\frac{\partial}{\partial t}\left[k\left(\frac{\partial v_z}{\partial x} - \frac{\partial v_x}{\partial z}\right)\right]_{\text{horiz. aver.}} &= \frac{dB}{dt}\left(-k^2 v + \frac{d^2 v}{dz^2}\right) \\ &= -g\alpha k^2 T\theta + \nu B\left(k^4 v - 2k^2\frac{dv^2}{dz^2} + \frac{d^4 v}{dz^4}\right) .\end{aligned} \tag{22}$$

Equation (22) can be written

$$\dot{B} = -h_4\nu k^2 \times\left\{B - \left[g\alpha k^2\theta \Big/ \nu k^4\left(v - \frac{2}{k^2}\frac{d^2 v}{dz^2} + \frac{1}{k^4}\frac{d^4 v}{dz^4}\right)\right]T\right\} , \tag{23}$$

where

$$h_4 = \left(v - \frac{2}{k^2}\frac{d^2 v}{dz^2} + \frac{d^4 v}{dz^4}\right) \Big/ \left(v - \frac{1}{k^2}\frac{d^2 v}{dz^2}\right) . \tag{24}$$

The coefficient of T on right-hand side of Eq. (23) can be expressed in a different way by taking into account the following relation, derived from Eqs. (126) and (127) of Ref. 1;

$$\nu k^4\left(v-\frac{2}{k^2}\frac{d^2v}{dz^2}+\frac{d^4v}{dz^4}\right)$$

$$=g\alpha\Delta_c\theta v\Big/\chi\left(\theta-\frac{1}{k^2}\frac{d^2\theta}{dz^2}\right). \tag{25}$$

where $\Delta_c=\Delta T_c/a$. By inserting Eq. (25) into Eq. (23), and putting $z=0$, I obtain

$$B=-h_4\nu k^2\left|B-(h_3\chi k^2/\Delta_c)T\right| . \tag{26}$$

The single-mode dynamics of the Rayleigh–Bénard instability is fully described by the set of nonlinear equations (17),(18), and (26) in the variables $\Delta(t),B(t)$, and $T(t)$. The constants h_j, with $j=1,\ldots,4$ have been computed by putting $k=k_c=3.117/a$, and using for $v(z)$ and $\theta(z)$ the solutions reported in Ref. 2. The obtained values are $h_1=16.68, h_2=44.13, h_3=2.20$, and $h_4=2.61$.

B. Soret-driven instability

The situation considered here is that of a liquid mixture, having $k_T>0$, which is heated from below. At small temperature differences ΔT, a constant vertical concentration gradient will arise, according to the Soret effect, so that

$$c(z)=\bar{c}+(k_T/T)(\Delta T/a)z .$$

Above the critical temperature difference ΔT_c, the system goes unstable. The theoretical results[7,8] indicate that no convective heat flux is originated by the Soret-driven instability if $\chi\gg D$, as it happens usually in liquid mixtures. It is therefore reasonable to assume that the temperature distribution inside the cell is not modified by the convective mass motion, and therefore, for any value of ΔT

$$T=\bar{T}-(\Delta T/a)z . \tag{27}$$

It is easy to verify with Eqs. (1)–(4) that this assumption makes the SDI problem formally identical to the RBI problem, with the concentration c playing the role of the temperature. The vertical component of the velocity v_z and the concentration c are expressed in the single-mode approach as

$$v_z=B(t)v'(z)\cos(\vec{k}\cdot\vec{r}) , \tag{28}$$

$$c=\bar{c}+A'(z,t)+C(t)w(z)\cos(\vec{k}\cdot\vec{r}) . \tag{29}$$

The dimensionless functions $v'(z)$ and $w(z)$ are different from $v(z)$ and $\theta(z)$ because the appropriate boundary condition for w is the analogous of Eq. (10) instead of Eq. (9). Indeed the condition of fixed temperatures of the plates implies, for the Soret cell, a fixed concentration gradient at the boundaries. I write $A'(z,t)$ as

$$A'(z,t)=\frac{k_T}{\bar{T}}\frac{\Delta T}{a}z-A(t)f'(z) , \tag{30}$$

where the dimensionless function $f'(z)$ must satisfy the boundary conditions $f'(0)=0$ and $df'/dz=0$ for $z=\pm\frac{1}{2}a$, and is given by

$$f'(z)=\int_0^z\frac{v'w}{a}dz . \tag{31}$$

Following the same procedure used for the RBI case, I obtain from Eqs. (1),(2), and (4) the set of equations

$$\dot{\Delta}'=(h_1/2a^2)BC-(h_2D/a^2)(\Delta'-\Delta'_0) , \tag{32}$$

$$\dot{C}=-\Delta'B-h_3Dk^2C , \tag{33}$$

$$\dot{B}=-h_4\nu k^2[B+(h_3Dk^2/\Delta'_c)C] , \tag{34}$$

where

$$\Delta'(t)=\frac{k_T}{\bar{T}}\frac{\Delta T}{a}-A(t)\left(\frac{df'}{dz}\right)_{z=0},$$

$$\Delta'_0=(k_T/\bar{T})(\Delta T/a) ,$$

$$\Delta'_c=(k_T/\bar{T})(\Delta T_c/a) ,$$

and the constants h_j's are defined as before by Eqs. (19)–(21) and (24), with f,θ, and v replaced by f',w, and v'. Note that Eqs. (32)–(34) are the same as Eqs. (17),(18), and (26), with Δ',C, and D instead of $\Delta,-T$, and χ. In the SDI case, as for the RBI with boundary conditions given by Eqs. (8) and (10), the minimum of the marginal-stability curve occurs for $k_c=0$, and the actual value of k is dependent on the finite width of the cell. Since the behavior of $v'(z)$ and $w(z)$ is influenced by k, one should conclude that the coefficients h_j's have no "universal" value, but depend on the actual geometry of the experiment. It should be noted that even in the RBI case discussed above, the independence of the h_j's from the geometry is limited probably to cells having large aspect ratios. An approximate evaluation of the h_j's for the SDI can be performed by choosing for $v'(z)$ and $w(z)$ the lowest-order polymonial expression which satisfies the boundary conditions, that is

$$v'(z)=1-8(z/a)^2+16(z/a)^4 ,$$

$w(z)=1$. One finds $h_1=h_2=10.91$, $h_3=1$. Furthermore, for small ka, $h_4=24/(ka)$.

As mentioned in the Introduction, the Soret-driven instability may also occur in a binary mixture having $k_T<0$, but heated from above, that is, with a negative temperature difference ΔT. It can be immediately verified that Eqs. (32)–(36) describe equally well this latter case.

III. STEADY-STATE SOLUTIONS

A. Rayleigh-Bénard instability

The steady-state solutions Δ_s,T_s, and B_s of Eqs. (17),(18), and (26), as obtained by putting

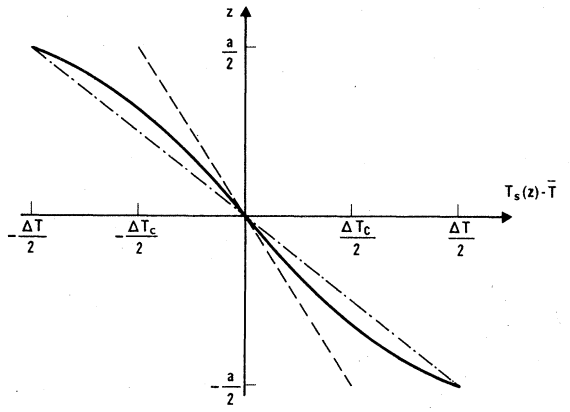

FIG. 1. Height dependence of the reduced horizontally averaged steady-state temperature $T_s(z)-\bar{T}$ in a fluid layer of thickness a, when the temperature difference ΔT between the plates is twice the threshold ΔT_c for the Rayleigh-Bénard instability. Note that the temperature gradient is equal to the critical temperature gradient at midheight, and is larger than $\Delta T/a$ at the boundary.

$\dot{\Delta}=\dot{T}=\dot{B}=0$, are

$$\Delta_s=\Delta_c=\Delta T_c/a\,, \tag{35}$$

$$T_s=\left(\frac{2h_2}{h_1h_3}\right)^{1/2}\frac{\Delta_c}{k}\epsilon^{1/2}=0.498\,T_c\epsilon^{1/2}\,, \tag{36}$$

$$B_s=\left(\frac{2h_2h_3}{h_1}\right)^{1/2}k\chi\epsilon^{1/2}=10.64\frac{\chi}{a}\epsilon^{1/2}\,, \tag{37}$$

where $\epsilon=(\Delta_0-\Delta_c)/\Delta_c$.

Expressions for T_s and B_s having the same structure as Eqs. (36) and (37) have already been derived by other authors,[4,24] with numerical constants about 10% larger than those given in Eqs. (36) and (37).

Equation (35) predicts that the horizontally averaged temperature gradient at the midplane of the cell takes, above threshold, a value independent of ΔT and coincident with the critical temperature gradient. This saturation effect does not seem to have been described in previous treatments of the RBI steady state. Furthermore, by using Eqs. (11), (13), and (35), the full vertical distribution of the horizontally averaged steady-state temperature $T_s(z)$ is derived, and reads

$$T_s(z)=\bar{T}-\frac{\Delta T}{a}z+\frac{\Delta T-\Delta T_c}{a}\frac{f(z)}{(df/dz)_{z=0}}\,. \tag{38}$$

The height dependence of $T_s(z)-\bar{T}$ for $\epsilon=1$ is shown in Fig. 1.

Heat-transfer measurements on the RBI are usually described in terms of the dependence of the Nusselt number on ΔT. The Nusselt number, defined as

$$\mathrm{Nu}=(Q_{\mathrm{conv}}+Q_{\mathrm{cond}})/Q_{\mathrm{cond}}\,,$$

where Q_{conv} and Q_{cond} are the convective and the conductive heat flux, respectively, can be expressed as

$$\mathrm{Nu}=a\left|dT/dz\right|_{z=a/2}\Delta T^{-1}\,,$$

and therefore one obtains from Eq. (38)

$$\mathrm{Nu}-1=\alpha(\Delta T-\Delta T_c)/\Delta T \tag{39}$$

where

$$\alpha=\frac{2H}{1-2H}\,,\quad H=\int_{-a/2}^{0}\frac{vw}{a}dz\,.$$

The numerical computation gives $H=0.311$ and $\alpha=1.65$. This latter value is 15% larger than both the theoretical[24] and the experimental[25] values reported for the case of two-dimensional rolls and large Prandtl number.

Accurate measurements of the velocity field of the RBI have been performed[26] by laser Doppler velocimetry, using a high-Prandtl-number liquid and a rectangular cell with a large aspect ratio. In the range $0<\epsilon<2$, two-dimensional rolls showing a sinusoidal dependence on the horizontal coordinate are found. In the range $2<\epsilon<10$ higher-order harmonics are necessary to describe the x dependence of the velocity amplitude. The amplitude of the fundamental mode is found to follow the law $\epsilon^{1/2}$, with a numerical proportionality constant slightly larger than that predicted by Eq. (37) and in good agreement with the calculations of Refs. 4 and 27.

B. Soret-driven instability

The steady-state solutions Δ'_s, C_s, and B_s of Eqs. (32)–(34) are

$$\Delta'_s=\Delta'_c=(k_T/\bar{T})(\Delta T_c/a)\,, \tag{40}$$

$$C_s=\left(\frac{2h_2}{h_1h_3}\right)^{1/2}\frac{\Delta'_c}{k}\epsilon^{1/2}$$

$$=1.41\frac{k_T}{ka}\frac{\Delta T_c}{\bar{T}}\epsilon^{1/2}\,, \tag{41}$$

$$B_s=-\left(\frac{2h_2h_3}{h_1}\right)^{1/2}kD\epsilon^{1/2}$$

$$=-1.41ka\frac{D}{a}\epsilon^{1/2}\,. \tag{42}$$

The expressions obtained in Sec. IV of Ref. 8 by a perturbation analysis seem to be quite different from Eqs. (41) and (42) apart from the expected $\epsilon^{1/2}$ dependence of C_s and B_s.

Since D is much smaller than χ for liquid mixtures, direct measurements of B_s are more difficult to perform in the SDI than in the RBI. However, the concentration modulation predicted by

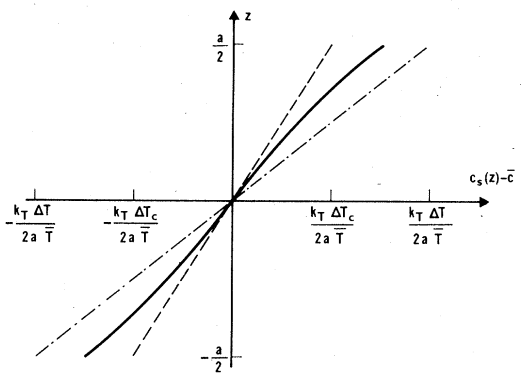

FIG. 2. Height dependence of the reduced horizontally averaged steady-state concentration $c_s(z)-\bar{c}$ in a binary liquid layer of thickness a, when the temperature difference ΔT between the plates is twice the threshold ΔT_c for the Soret-driven instability. Note that the concentration gradient is equal to the critical concentration gradient at midheight, and is not affected by the convective mass motion at the boundary.

Eq. (41) is quite large, and certainly measurable by the beam-deflection technique described in Refs. 11 and 12.

Equation (40) predicts for the horizontally averaged concentration gradient the same saturation effect described above for the temperature gradient. Therefore all the considerations developed with regard to Eq. (35) could be repeated here. The vertical distribution of the horizontally averaged concentration $c_s(z)$ reads

$$c_s(z)=\bar{c}+\frac{k_T}{\bar{T}}\frac{\Delta T}{a}z-\frac{k_T}{a}\times\frac{\Delta T-\Delta T_c}{\bar{T}}\frac{f'(z)}{df'/dz|_{z=0}}. \tag{43}$$

The height dependence of $c_s(z)-\bar{c}$ for $\epsilon=1$ is shown in Fig. 2.

Following the analogy with the RBI case, one can define here the dimensionless quantity

$$a\left|\frac{dc_s}{dz}\right|_{z=-a/2}\Delta c^{-1},$$

where $\Delta c=c_s(\frac{1}{2}a)-c_s(-\frac{1}{2}a)$. Such a quantity represents the ratio between the true thermal diffusion ratio and the apparent thermal diffusion ratio. Since mass convection partially destroys the concentration gradient due to thermal diffusion, the ratio defined above is larger than 1 above threshold. From Eq. (43) the following expression is derived:

$$a\left|\frac{dc}{dz}\right|_{z=-a/2}\Delta c^{-1}=\frac{1}{1-\alpha'(1-\Delta T_c/\Delta T)}, \tag{44}$$

where

$$\alpha'=2\int_{-a/2}^{0}\frac{v'w}{a}dz.$$

By using the approximate expressions for v' and w given in Sec. II B, I obtain $\alpha'=\frac{8}{15}\cong 0.53$.

The prediction, expressed by Eq. (40), that the horizontally averaged concentration gradient at midheight is locked, above threshold, to the critical value is in very good agreement with the measurements performed by Giglio and Vendramini[11] for the SDI in the mixture ethanol-toluene. The results reported in Fig. 1 of their paper show indeed that $\Delta_s=\Delta_c$ above threshold. The measurements performed by the same authors on the SDI in a aqueous solution of polyvinylalcohol[12] show an increase of the midheight concentration gradient with ΔT. It should however be considered that the beam-deflection technique averages the concentration gradient over a vertical range which coincides with the diameter d of the laser beam. In the case of the experiment described in Ref. 12, d is about 1 mm and is not negligible in comparison with $a=5$ mm. It is easy to compute from Eq. (44) the average of the concentration gradient over the range $(-\frac{1}{10}a,+\frac{1}{10}a)$. The result is

$$(\Delta_s')_{av}=k_T(T_c/\bar{T})(1+\tfrac{4}{15}\epsilon),$$

in very good agreement with the experimental data shown in Fig. 1 of Ref. 12.

IV. TRANSIENT SOLUTIONS

Equations (17), (18), and (26) fully describe the transient evolution of the RBI toward the steady state starting from an arbitrary initial condition at $t=0$. Similarly, Eqs. (32)–(34) describe SDI transients. In many relevant cases the description of the transient can be considerably simplified by using the so-called adiabatic approximation which is based upon the comparison of the different time scales involved in the problem and the consequent elimination of the faster variables. I discuss here for simplicity only the case $\nu/\chi\gg 1$ (large Prandtl number) for the RBI and $\nu/D\gg 1$ for the SDI, since these are the cases investigated in all the experiments published so far about instability transients, except for the experiment performed on liquid helium.[18] Under these assumptions the fast variable is B (B' for the SDI), and the variable showing critical slowing down is T (C for the SDI). In the region very close to threshold ($\epsilon\ll 1$), also the dynamics of Δ (or Δ') is fast in comparison with that of T (or C), and therefore both B (or B') and Δ (or Δ') can be adiabatically eliminated by putting $\dot{B}=\dot{\Delta}=0$.

The resulting dynamic equation for T is

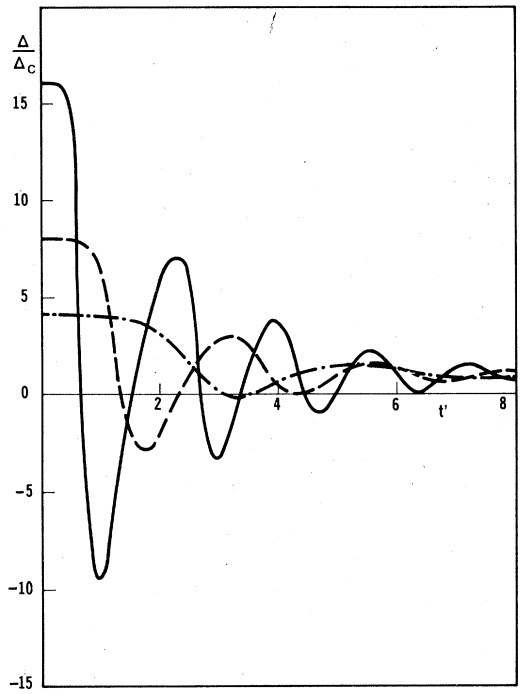

FIG. 3. Time evolution of the normalized temperature gradient Δ/Δ_c starting from the initial condition $\Delta(0)=\Delta_0$ for three distinct values of $\epsilon=(\Delta_0-\Delta_c)/\Delta_c$; $\epsilon=3$ (dot-dashed line), $\epsilon=7$ (dashed line), and $\epsilon=15$ (full line). The normalized time t' is defined as $t'=(h_2\chi/a^2)t$.

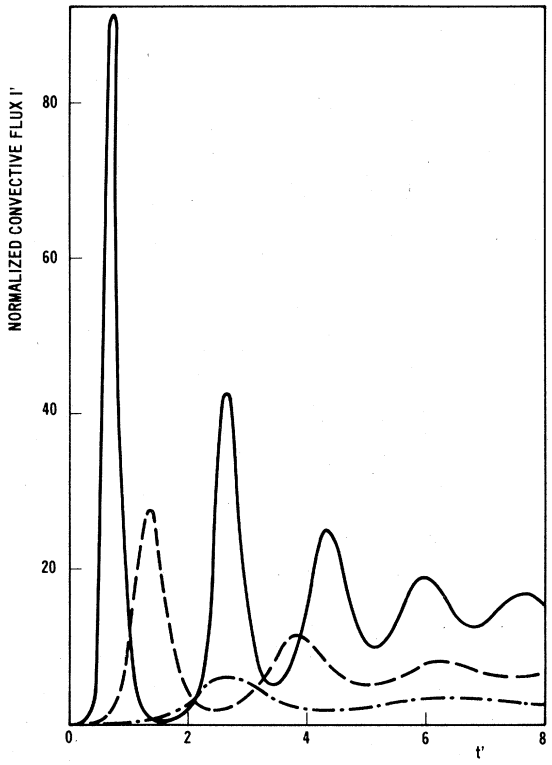

FIG. 4. Time evolution of the normalized convective flux $I'=(h_1/2h_2\chi\Delta_c)\,I$, starting from the initial condition $I'(0)=10^{-2}$ for the same three values of ϵ used in Fig. 3.

$$\dot{T}=h_3\chi k^2\epsilon T-\frac{h_1h_3^2}{2h_2}\frac{\chi k^4}{\Delta_c^2}T^3. \tag{45}$$

Equation (45) is a Van der Pol equation, such as the equation describing the dynamics near threshold of electronic and optical oscillators.[28] The solution of Eq. (45) is well known[23] and it will not be discussed here. I simply note that the time constant τ for the decay of small deviations form the steady state, as derived from Eq. (45), is $\tau=\tau_0\epsilon^{-1}$, where $\tau_0=(h_3\chi k^2)^{-1}=0.047\,a_2/\chi$. The obtained τ_0 is in good agreement with the theoretical and experimental results reported in Ref. 17 for the same boundary conditions discussed in this paper.[29,30]

The dynamics near threshold of the SDI is described by the same Eq. (45) where T is substituted by C, and χ by D. The constant τ_0 is given by $\tau_0=a^2/h_3k^2a^2D$. As noted in Sec. II, the actual value of ka depends on the geometry of the experiment, and therefore τ_0 has no universal numerical value for the SDI. The only available SDI experimental data for τ are those of Ref. 12, where it is found $\tau_0\simeq 20a^2/\pi^2D$. The comparison of this relation with the theoretical formula gives $ka\simeq 0.7$.

Slightly above threshold, when τ cannot be considered much larger than the characteristic evolution time of the temperature gradient which is $(\chi h_2/a^2)^{-1}$, it is not possible to eliminate adiabatically Δ. The single condition $\dot{B}=0$ leads to the following pair of equations:

$$\Delta=-(h_1/a^2)I-(h_2\chi/a^2)(\Delta-\Delta_0), \tag{46}$$

$$\dot{I}=(2h_3\chi k^2/\Delta_c)(\Delta-\Delta_c)I, \tag{47}$$

where $I=\frac{1}{2}BT$ represents the convective heat flux at the midplane of the liquid layer. Note that, under the assumption $\dot{B}=0$, I is proportional to T^2 and to B^2.

Of course, the same Eqs. (46) and (47) hold for the SDI, with the substitution of Δ' and D, to Δ and χ, and with $I=-\frac{1}{2}BC$ representing the convective mass flux.

By introducing the dimensionless variables $t'=\chi(h_2/a^2)t$, $x=\Delta/\Delta_c$, and $I'=Ih_1/(h_2\chi\Delta_c)$, Eqs. (46) and (47) become

$$\dot{x}=-I'-(x-x_0), \tag{48}$$

$$\dot{I}'=hI'(x-1), \tag{49}$$

where $h=(2h_3/h_2)k^2a^2$. For the RBI, $ka=3.117$,

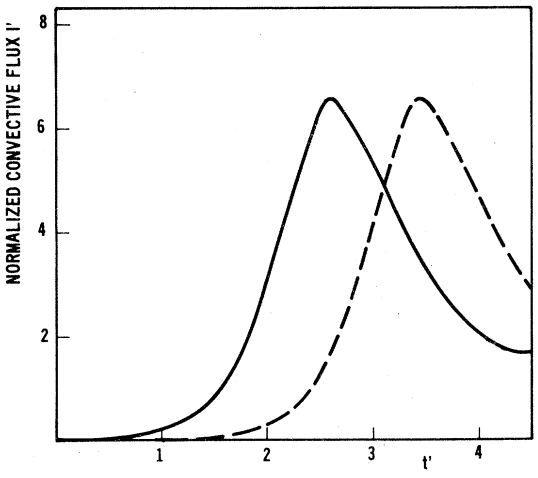

FIG. 5. Time evolution of the normalized convective flux $I' = (h_1/2h_2\gamma\Delta_c)\, I$, for $\epsilon = 3$, with the initial conditions $I'(0) = 10^{-2}$ (full line), $I'(0) = 10^{-3}$ (dashed line).

$h_2 = 44.13$, $h_3 = 2.20$, and therefore $h = 0.97$. For the SDI, h depends on the experimental parameters. If I take $ka = 0.7$, $h_2 = 10.91$, and $h_3 = 1$, I obtain $h = 0.09$.

The evolutions of Δ and I have been obtained by numerical computation[31] of Eqs. (48) and (49) with the initial conditions $\Delta(0) = \Delta_0$ and $I(0) = I_i$, where I_i is a small value simulating the noise which triggers the onset of the instability. Some evolutions, obtained for three distinct values of ϵ, and for $h = 1$ (RBI case) are shown in Figs. 3 and 4. The most interesting and new feature of the transients is the damped oscillatory approach to steady state shown for not too small ϵ. The curves relative to large values of ϵ are particularly striking because the gradient Δ goes through a negative peak and the convective flux has an overshoot several times larger than the steady-state value.

It should be noted that the choice of I_i does not influence the shape of the transient, as long as I_i is much smaller than the steady-state value I_s. Indeed it is easy to see from Eqs. (46) and (47) that I grows exponentially for short times with a time constant $2\tau(2h_3\chi k^2\epsilon)^{-1}$. A reduction of I_i by a factor γ is therefore simply equivalent to introducing a delay of $2\tau \ln\gamma$ in the transient. An illustration of this effect is reported in Fig. 5. It is interesting to note that a measurement of the time delay of the transient may allow to evaluate the thermal-noise contribution to the convective mode in the system before the switching-on operation.

Some information about the damped oscillating behavior can be gained by a linearization of Eqs. (46) and (47) around the steady state. The associated characteristic equation possesses two complex-conjugate roots when $\epsilon > \epsilon_t$. The threshold for the appearance of oscillations is $\epsilon_t = h_2/8h_3k^2a^2$, the expression of the period of the oscillations is

$$\epsilon_{osc} = (2a^2k^2h_2h_3/\pi^2)^{-1/2}(a^2/\chi)(\epsilon - \epsilon_t)^{-1/2},$$

and the damping time of the oscillations is $\tau_D = 2(\chi h_2/a^2)^{-1}$.

Few experiments have been performed on the transient behavior of the RBI. The verification of the theoretical evolutions requires a fast-switching technique, which would be analogous to the well-known Q switching of lasers. Fast means that the uniform temperature gradient Δ_0 must be applied to the fluid layer in a time interval much shorter than the rise time τ of the convective flux. Since the time constant for heat diffusion across the layer is about τ_0, in the usual experimental configurations the switching is fast only in the region slightly above threshold where $0 < \epsilon < 1$. An interesting method for preparing the system with a large temperature gradient ($\Delta_0 \gg \Delta_c$) and no convective motion is that used by Sawada[19] who operates at $t = 0$ a sudden flip of configuration from $\vec{g} \uparrow\uparrow \text{grad}\, T$ to $\vec{g} \uparrow\downarrow \text{grad}\, T$.

Damped oscillatory transients have been experimentally observed by Bergé and Dubois,[16] and by Sawada.[19] All the qualitative features are correctly predicted by Eqs. (46) and (47). The empirical law

$$\tau_{osc} = 200\,\epsilon^{-0.45\pm0.05}$$

proposed in Ref. 16 is in good agreement with the expression for τ_{osc} written above, taking into account that $\epsilon_t = 0.2$ for the RBI case and that $P = \nu/\chi = 130$ for that experiment.

The only reported study on SDI transients is that of Ref. 12, where also damped oscillatory transients have been observed not too close to threshold. Preliminary measurements of τ_{osc} for the SDI in the range $2 < \epsilon < 8$ are in agreement with the predicted power-law dependence.[32]

V. LORENZ MODEL AND ANALOGY WITH THE LASER

The reduction of the hydrodynamic conservation equations for a single-component system to a simple set of three time-dependent equations is a result which can already be found in the so-called Lorenz model of the RBI.[20] Equations (17), (18), and (26) can indeed be considered as a generalization of the Lorenz equations to the case of non-sinusoidal vertical dependence of the horizontally averaged temperature and velocity. In fact, by introducing the dimensionless variables

$$t' = h_3\chi k^2 t\,,$$

$$X = (\tfrac{1}{2}h_1)^{1/2}B/h_3\chi k^2 a\,,$$

$$Y = (\tfrac{1}{2}h_1)^{1/2}T/a\Delta_c\,,$$

and

$$Z=(\Delta_0-\Delta)/\Delta_c\,,$$

and the new constants $\tilde{P}=(h_4/h_3)P$ and $b=h_2/h_3k^2a^2$, the three equations become

$$\dot{X}=-\tilde{P}(X-Y)\,, \tag{50}$$

$$\dot{Y}=-XZ-Y+(\epsilon+1)X\,, \tag{51}$$

$$\dot{Z}=XY-bZ\,. \tag{52}$$

The only difference between Eqs. (50)–(52) and the Lorenz equations lies in the expressions for $\tilde{P}$ and b which contain the coefficients h_j. These coefficients, as shown in Sec. II, depend on turn upon $v(z)$ and $\theta(z)$. The assumption made in the Lorenz model that $v(z)$ and $\theta(z)$ are sinusoidal is not consistent with the boundary conditions actually imposed in real experiments. The treatment presented in this paper shows that a generalized Lorenz model describes correctly the region of regular convection of the RBI and can be equally well applied to the SDI.

Interest in the Lorenz model has been so far due to the fact that Lorenz equations seem to give a randomly fluctuating time response when τ is larger than a threshold value ϵ_{tt}. Such a behavior is thought to be connected with the problem of turbulence.[20] The expression of ϵ_{tt} is derived by linearization of Eqs. (50)–(52) around the steady-state solutions $X=Y=\pm\sqrt{b\epsilon}$, $Z=\epsilon$. The resulting characteristic equation possesses one real negative root and two complex-conjugate roots which are pure imaginary if $\epsilon=\epsilon_{tt}$, where

$$\epsilon_{tt}=\tilde{P}(\tilde{P}+b+3)(\tilde{P}-b-1)^{-1}-1\,. \tag{53}$$

Note that, if $\tilde{P}$ is much larger than 1, $\epsilon_{tt}\simeq\tilde{P}$. Several RBI experiments performed in high-Prandtl-number fluids have indeed shown the flow begins to oscillate in time as ϵ is increased above a threhold value.[16,33] The reported thresholds are close to $\tilde{P}$. Such an agreement may be fortuitous because the approximations used to derive Eqs. (50)–(52) limit the validity of the treatment to ϵ smaller than $\tilde{P}$.

As noted by Haken,[21] the Lorenz equations are identical to the Maxwell–Bloch equations which describe the dynamics of a single-mode laser for a resonant-field–atom interaction. The dimensionless velocity X plays the role of the electric field amplitude, Y represents the atomic polarization, and Z the population inversion. Analogies among different instabilities in the region very close to threshold are now well established.[14] The interesting feature of the analogy between the Lorenz model of the RBI and the single-mode laser model is that it holds for arbitrary values of the pump parameter, and not only for $\epsilon\ll 1$.

The most common situation in real lasers is that the relaxation time T_2 of the polarization is much shorter than both the relaxation time T_1 of the population inversion and the field decay time τ_c. Using the notation of Eqs. (50)–(52), this means both $\tilde{P}$ and b much smaller than 1.[34] In such a case, it is usual to eliminate adiabatically the polarization. Also the case $\tau_c\ll T_1, T_2$ has received considerable attention in quantum optics.[22,35] The adiabatic elimination of the "fast" variable X allows to derive the equations describing superradiant pulses. The approximation $B=0$ used to obtain Eqs. (46) and (47) clearly corresponds to the superradiant case. The analogy suggests the possibility of observing giant pulses in the transient regime of convective instabilities by performing the experiment with a single-component fluid having a large Prandtl number, or a two-component liquid having a large ν/D ratio. When ϵ is much larger than 1 (but still smaller than $\tilde{P}$), the "superradiant" pulse in the convective flux has a temporal width $\tau=(h_3\chi k^2\epsilon)^{-1}$, and a peak value

$$I_p=h_1\epsilon^2/2\chi k^2a^2\Delta_c\,.$$

An other suggestion stemming from the analogy with the laser is the possibility of studying pretransitional phenomena in the homogeneous regime preceding the convective transition. In analogy to phase transitions in thermal equilibrium, theory predicts an increase in the magnitude of thermally excited fluctuations of the unstable modes.[36] In principle, the experiment should run as follows. The liquid layer is first prepared at the state near threshold (ϵ slightly below to zero) whose fluctuations one wants to measure. At $t=0$ the temperature difference across the layer is suddenly brought to a value ΔT well above threshold ($\epsilon>1$). The system evolves toward the new steady state with a transient whose shape depends only on ΔT. The time lag of the transient depends, however, on the fluctuation present at $t=0$, as discussed in Sec. IV and shown in Fig. 5. The proposed experiment is of course a statistical experiment.[23] For each initial position, the observation of the transient should be repeated a sufficient number of times to obtain a significant average.

VI. CONCLUDING REMARKS

I have discussed in this paper the steady state and the dynamics of both the Rayleigh–Bénard and the Soret-driven instabilities. The main assumptions used to derive the basic equations are (i) the usual Boussinesq–Oberbeck model, (ii) two-dimensional rolls with sinusoidal horizontal dependence and with a wavelength independent of ΔT,

and (iii) $\chi/D \gg 1$ for the SDI. The numerical constants are calculated by assuming rigid-rigid boundary and fixed-plate temperatures.

A quantitative theoretical explanation is found to recent experimental results, such as the saturation of the horizontally averaged concentration gradient at $z = 0$ in the SDI, the appearance of relaxation oscillations in RBI and SDI transients and the dependence of the oscillation period on ΔT. Several other features of the theoretical results need an experimental verification.

Some experiment is suggested by the analogy with the laser. In particular, the statistical measurement of the time jitter of the convective-instability transient appears as the only practical way to obtain information on pretransitional fluctuations of the unstable mode. The main difficulty in such an experiment is probably to get rid of all the external disturbances which might obscure the small intrinsic fluctuations one wishes to observe.

ACKNOWLEDGMENTS

Thanks are due to M. Giglio for many illuminating discussions, and to the Centro Informazioni Studi Esperienze Computer Center for help in the numerical computations with the GOSPEL program.

This work was supported by Consiglio Nazionale delle Ricerche–Centro Informazioni Studi Esperienze Contract No. 78.00901.02.

---

*Researcher from the Italian National Research Council (CNR).

[1]V. Degiorgio, Phys. Rev. Lett. 41, 1293 (1978).
[2]S. Chandrasekhar, *Hydrodynamic and Hydromagnetic Stability* (Oxford University, London, 1961), Chap. II.
[3]E. L. Koschmieder, Adv. Chem. Phys. 26, 177 (1974).
[4]C. Normand, Y. Pomeau, and M. G. Velarde, Rev. Mod. Phys. 49, 581 (1977).
[5]F. H. Busse, Rep. Prog. Phys. 41, 1929 (1978).
[6]G. Z. Gershuni and E. M. Zhukhovitskii, Prikl. Mat. Mech. (U.S.S.R.) 27, 1197 (1963); D. T. J. Hurle and E. Jakeman, J. Fluid. Mech. 47, 667 (1971).
[7]R. S. Schechter, I. Prigogine, and R. Hamm, Phys. Fluids 15, 379 (1972).
[8]M. G. Velarde and R. S. Schechter, Phys. Fluids 15, 1707 (1972).
[9]S. R. De Groot and P. Mazur, *Non-Equilibrium Thermodynamics* (North-Holland, Amsterdam, 1962), Chaps. 7, 8, 11.
[10]A. Sparasci and J. H. V. Tyrrell, J. Chem. Soc. Faraday I, 71, 42 (1975).
[11]M. Giglio and A. Vendramini, Opt. Commun. 20, 438 (1977).
[12]M. Giglio and Vendramini, Phys. Rev. Lett. 39, 1014 (1977).
[13]W. R. Lamb, Phys. Rev. 134, A1429 (1964); see also H. Haken and H. Sauermann, Z. Phys. 176, 47 (1963).
[14]H. Haken, *Synergetics* (Springer-Verlag, Berlin, 1978).
[15]J. T. Stuart, J. Fluid Mech. 4, 1 (1958).
[16]P. Bergé and M. Dubois, Opt. Commun. 19, 129 (1976).
[17]J. Wesfreid, Y. Pomeau, M. Dubois, C. Normand, and P. Bergé, J. Phys. (Paris) 39, 725 (1978).
[18]R. B. Behringer and G. Ahlers, Phys. Lett. 62A, 329 (1977).
[19]Y. Sawada, Phys. Lett. 65A, 5 (1978).
[20]E. N. Lorenz, J. Atmos. Sci. 20, 130 (1963); J. B. McLaughlin and P. V. Martin, Phys. Rev. A 12, 186 (1975).
[21]H. Haken, Phys. Lett. 53A, 77 (1977).
[22]R. Bonifacio and P. Schwendimann, Lett. Nuovo Cimento 3, 509 (1970).
[23]Statistical measurements on single-mode laser transients are reported by F. T. Arecchi, V. Degiorgio, and B. Querzola [Phys. Rev. Lett. 19, 1168 (1967)] and F. T. Arecchi and V. Degiorgio [Phys. Rev. A 3, 1108 (1971)].
[24]A. Schlüter, D. Lortz, and F. H. Busse, J. Fluid Mech. 23, 129 (1965).
[25]E. L. Koschmieder and S. G. Pallas, Int. J. Heat Mass Transfer 17, 991 (1974).
[26]M. Dubois and P. Bergé, J. Fluid Mech. 85, 641 (1978).
[27]F. H. Busse, J. Math. Phys. 46, 140 (1967).
[28]A laserlike approach to the RBI, limited to $\epsilon \ll 1$, which leads to Eq. (45) and allows a thorough discussion of fluctuations is discussed by R. Graham, in *Fluctuations, Instabilities, and Phase Transitions*, edited by T. Riste (Plenum, New York, 1975), p. 215.
[29]A measurements of τ in the pretransitional region has been recently reported by C. Allain, H. Z. Cummins, and P. Lallemand [J. Phys. Lett. (Paris) 39, L473 (1978)].
[30]The time constant τ_0 relative to the free-free boundary condition is calculated for the RBI by R. Graham (see Ref. 28) and by H. N. W. Lekkerkerker and J. P. Boon [Phys. Rev. A 10, 1355 (1974)]; for the SDI, see H. N. W. Lekkerkerker and W. G. Laidlaw, J. Phys. (Paris) 38, 1 (1977).
[31]A new interactive program, GOSPEL, developed by the Centro Informazioni Studi Esperienze computer center, was used. See A. Brini, R Ferrari, T. Montagna, M. Montagni, G. Perna, and J. Szanto, in *International Computing Symposium 1977*, edited by E. Morlet and D. Ribbens (North-Holland, Amsterdam, 1977) p. 271.
[32]M. Giglio and A. Vendramini (private communication).
[33]G. E. Willis and J. W. Deardorff, J. Fluid Mech. 44, 661 (1970); F. H. Busse and J. A. Whitehead, *ibid.* 66, 67 (1974).
[34]Note that b cannot be larger than 1 for the laser model.
[35]See, for instance, R. Bonifacio, M. Gronchi, L. A. Lugiato, and A. M. Ricca, in *Coherence and Quantum Optics IV*, edited by L. Mandel and E. Wolf (Plenum, New York, 1978), p. 939, and references quoted therein; V. Degiorgio, Opt. Commun. 2, 362 (1971).
[36]V. M. Zaitsev and M. L. Shliomis, Sov. Phys. JETP 32, 866 (1971); see also the papers mentioned in Refs. 28 and 29.